International Journal of Minerals, Metallurgy and Materials
Volume 27, Number 2, February 2020, Page 152
https://doi.org/10.1007/s12613-019-1936-0

An experimental study on size distribution and zeta potential of bulk cavitation nanobubbles

Xu-yu Zhang[1)], *Qian-shuai Wang*[1)], *Zhong-xian Wu*[1)], *and Dong-ping Tao*[1,2)]

1) School of Mining Engineering, University of Science and Technology Liaoning, Anshan 114051, China
2) School of Resources and Environmental Engineering, Shandong University of Technology, Zibo 255049, China
(Received: 12 September 2019; revised: 19 October 2019; accepted: 25 October 2019)

Abstract: Nanobubble flotation technology is an important research topic in the field of fine mineral particle separation. The basic characteristics of nanobubbles, including their size, concentration, surface zeta potential, and stability have a significant impact on the nanobubble flotation performance. In this paper, bulk nanobubbles generated based on the principle of hydrodynamic cavitation were investigated to determine the effects of different parameters (e.g., surfactant (frother) dosage, air flow, air pressure, liquid flow rate, and solution pH value) on their size distribution and zeta potential, as measured using a nanoparticle analyzer. The results demonstrated that the nanobubble size decreased with increasing pH value, surfactant concentration, and cavitation-tube liquid flow rate but increased with increasing air pressure and increasing air flow rate. The magnitude of the negative surface charge of the nanobubbles was positively correlated with the pH value, and a certain relationship was observed between the zeta potential of the nanobubbles and their size. The structural parameters of the cavitation tube also strongly affected the characteristics of the nanobubbles. The results of this study offer certain guidance for optimizing the nanobubble flotation technology.

Keywords: nanobubble; hydrodynamic cavitation; zeta potential; size distribution

1. Introduction

The term "nanobubbles" generally refers to tiny bubbles with a bubble diameter less than 1 μm, which are nanoscale gaseous aggregates existing at the solid–liquid interface or in the liquid-phase environment; by contrast, microbubbles often have a diameter between 1 and 1000 μm [1]. Nanobubbles have characteristics that differ from those of conventional air bubbles and are widely used in mineral flotation, sewage treatment, targeted drug delivery, biomedicine, nanomaterials, and other industrial fields. Four cavitation-based methods are available to generate microbubbles and/or nanobubbles: hydrodynamic cavitation, ultrasonic cavitation, optical cavitation, and particle cavitation [2]. The hydrodynamic cavitation method is most commonly used in engineering applications because of its relative equipment simplicity, convenient implementation, low energy consumption, and low maintenance costs [3–8]. In the present paper, the basic characteristics of nanobubbles produced by this method are studied.

Although their size and gas type differ, bubbles play important roles in different fields. For example, Madavan *et al.* [9] used microbubbles generated with a perforated plate jet device to reduce the local friction of the plate by approximately 80%. They also reported that the drag reduction effect was related to the pore diameter. Microbubbles are widely used in the treatment of oily wastewater, municipal wastewater, and industrial wastewater because of their high adsorption rate [10–11]. In the field of flotation, nanobubbles are characterized with a small particle size, large specific surface area, and long existence time. By increasing the collision and adhesion probability between particles and bubbles and reducing the probability of particle detachment from bubbles, the flotation kinetics can be substantially improved and the flotation effect can be enhanced [6,8,12–15]. In the field of agriculture, the oxygen content in a water body can be increased by introducing air or oxygen into the water body using the aeration method with a micro/nanobubble generation device [16]. Nanobubble water with a high oxy-

Corresponding author: Dongping Tao E-mail: dptao@qq.com

gen content also has special properties related to sterilization, oxidation, and electrification and can promote plant growth, delay plant root senescence, and improve soil quality [17]. Nanobubbles can also solve the problem of anoxia in artificial fish ponds and reduce the content of nitrogen and phosphorus in water [18]. Cavitation bubbles are widely used in neutron detectors (e.g., helium tubes) to monitor leakage of nuclear materials [19]. Nanobubbles have strict requirements for size when used in medicine; they can be used in ultrasound imaging and intracellular drug delivery and to enhance the sensitivity of cancer cells to drugs [20–21].

The size of nanobubbles reflects their special properties to some extent. The rising velocity of bubbles is known to be related to bubble size. When the bubble size is less than 10 μm, bubbles begin to show some special physical and chemical characteristics such as slower rising or even settling and long duration times. The smaller bubble size and larger specific surface area provide sufficient contact area for reaction with the particles. The zeta potential of the surface of nanobubbles can affect their stability in water. Therefore, the diameter and surface potential of nanobubbles are important topics of nanobubble characterization. Etchepare *et al.* [22] used a centrifugal multiphase pump (CMP) and a needle valve to study the influence of the time interval and pressure on the concentration and diameter of nanobubbles through pressurization, demonstrating the high stability and long life of nanobubbles generated by their nanobubble water dispersion system. Fan *et al.* [23] analyzed and tested the particle sizes of nanobubbles generated under different conditions using a homemade nanobubble generation system and found that the diameters of nanobubbles are mostly distributed between 191 and 800 nm. Najafi *et al.* [24] produced bulk nanobubbles with an average size of 290 nm through temperature changes in a closed container and also measured their zeta potentials. Their results showed that the zeta potentials of nanobubbles were consistent with those of larger bubbles.

A number of bubble size measurement techniques have been developed, including X-ray techniques [25], optical microscope and camera methods [26], a laser pulse method [27], a fluid dynamics method [28], resistivity, and image analysis [29–30]. Although image analysis is the most widely used method to characterize nanobubbles, it has some obvious disadvantages. For example, a transparent barrier is required for image acquisition, a low bubble concentration should be used, and the experimental setup is complicated. Even experiments with cameras equipped with modern high-speed charge-coupled devices are time consuming [31–32]. Therefore, using laser diffraction technology, i.e., dynamic light scattering technology, to measure bubble diameter has become the preferred research method.

Previous research on bulk nanobubbles has mainly focused on their role in industrial applications; research on the characteristics of nanobubbles themselves has not been comprehensive. In this paper, dynamic light scattering and other technologies are used to study important characteristics such as the size distribution, surface potential, and the stability of bulk nanobubbles generated via the hydrodynamic cavitation method. The effects of frother type and concentration, solution pH value, hydrodynamic cavitation conditions (air pressure, liquid flow rate of the cavitation tube, air flow rate, and internal structural parameters of the cavitation tube), and other factors on the characteristics of nanobubbles were investigated in depth, providing a scientific basis for fully understanding the mechanism and performance of nanobubbles in enhancing mineral flotation.

2. Experimental

2.1. Materials

One of the nonionic surfactants used in the test was methyl isobutyl methanol (MIBC), with a molecular weight of 102.2 g/mol and a purity of 99%. The other nonionic surfactant, n-pentanol, has a molecular weight of 88.15 g/mol and was of analytical purity. Anionic surfactant sodium oleate, with a molecular weight of 304.44 g/mol, was of chemical purity. HCl and NaOH used to adjust the pH value were also of analytical purity. In addition, the water used in this experimental study was deionized water with a conductivity of 0.14 μS/cm, produced by an ultrapure water system from Shenyang Xinjie Technology Co., Ltd.

2.2. Generation and size measurement of nanobubbles

The device for generating and measuring nanobubbles is shown in Fig. 1. A homemade hydrodynamic cavitation tube was used as a nanobubble generating device, and a circulating closed-circuit system was formed by connecting a circulating water pump (New Territories 25WBZ6-18) and a homemade cavitation tube through a plastic pipe with an inner diameter of 11 mm.

The efficiency of hydrodynamic cavitation is affected by many parameters, including the inlet pressure, physical and chemical properties of the liquid, structure of cavitation tube, and the solubility of the gas. When liquid flows at a high speed, hydrodynamic cavitation will occur because the pressure at a certain point drops below the vapor pressure instantaneously [33]. When the liquid flows through the throat of the cavitation tube at a certain speed, the speed of the liquid increases rapidly and the pressure of the liquid decreases sharply, thus generating a certain pressure difference

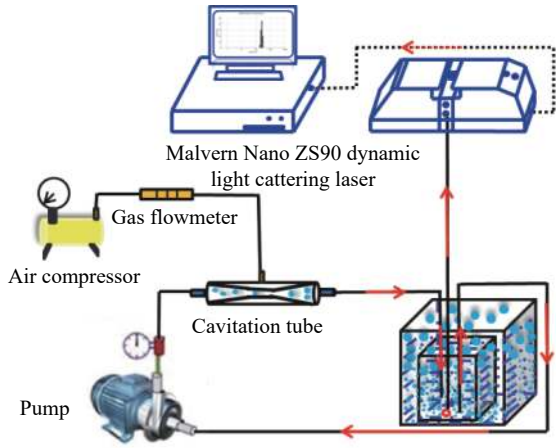

Fig. 1. Schematic of the nanobubble generation and size and the potential measuring system.

and finally generating a large number of nanobubbles. To induce high-intensity cavitation, the outlet pressure of the pump should be high. The suction of the circulating water pump makes the aqueous solution containing frothing agent flow through the specially designed cavitation tube where the internal pressure of the liquid flow is lower than the saturated vapor pressure of dissolved gas and the gas nuclei are precipitated in the form of nanobubbles.

To eliminate the influence of larger bubbles rising in the measurement process and to control the nanobubble concentration in water for optimum laser size analysis, the nanobubble reservoir at the right bottom of Fig. 1 consisted of an inner cell and an outer cell. The inner cell had a small hole for nanobubbles to diffuse to the outer cell to form a dilute nanobubble solution that was used as the sample for laser size analysis. The inner cell solution had a nanobubble concentration that was too high to be used directly for laser size analysis. The nanobubble solution in the outer cell was transferred to the size analyzer using a peristaltic pump or transferred manually using a pipette.

The bubble size detection device used in this study was a Malvern Nano ZS 90 particle size potential analyzer with a particle size measurement range from 2 to 36 μm. According to Mie's theory [34–35], the refractive indexes of bubbles and water were set to 1.0 and 1.33, respectively, and the size was measured at 22°C. Fifteen milliliters of cavitation solution was collected for measurement, and each group of samples were measured three times, with the average value being taken as the final value.

2.3. Zeta potential measurements

The surface zeta potential of nanobubbles was measured using a zeta potential analyzer (Malvern Nano ZS 90) to characterize the surface charge of nanobubbles in solution under different conditions. The bubble size for surface potential measurement ranged from 5 nm to 10 μm; each measurement was repeated three times, and the average was taken as the final value of zeta potential under a given condition.

3. Results and discussion

3.1. Effect of frother dosage on nanobubble size and zeta potential

The presence of frother affects the number and size of bubbles and it is necessary to investigate the effect of frother dosage on the size of bubbles. Fig. 2 shows the variation of nanobubble size as a function of the concentration of frother (MIBC) at 10, 20, 30, 40, and 50 mg/L.

Fig. 2 shows that the average size of nanobubbles is negatively correlated with the concentration of MIBC. When the dosage of MIBC was increased from 10 to 50 mg/L, the peak value in the particle size distribution was observed to shift toward smaller particle sizes and the average size of the nanobubbles decreased from 248 to 154 nm. Finch *et al.* [36] showed that increasing frother concentration can reduce surface tension and thus reduce bubble size. Azgomi [37] explained the effect of frother on bubble size on the basis of the mechanism of bubble coalescence prevention. He speculated that the frother molecules at the air–liquid interface formed hydrogen bonds with water, making the liquid film on the bubble surface more stable and thereby preventing bubble coalescence and reducing bubble size. Notably, surface tension is not the only factor that affects bubble size. Gupta *et al.* [38] studied the relationship between bubble size and surface tension in the presence of two frothers: MIBC and DF-1012. They demonstrated that, when DF-1012 was used as a frother, the bubble size was larger than when MIBC was used at the same concentration although its surface tension was lower. Moyo *et al.* [39] also found that adding some salt to the aqueous solution reduced bubble size but increased bubble surface tension.

Electrostatic force plays an important role at the gas–liquid–solid interface; thus, measurement of the zeta potential of bubbles is indispensable. However, researchers in the research field of froth flotation devote more attention to the charge on the surface of solid particles; very little research has been conducted on the surface charge of bubbles. Fig. 3 shows the change in zeta potential of nanobubbles when the MIBC concentration was varied from 0 to 50 mg/L.

The zeta potential decreased substantially as the nonionic surfactant (MIBC) concentration was increased from 0 to 10 mg/L in the solution but leveled off thereafter. Karraker

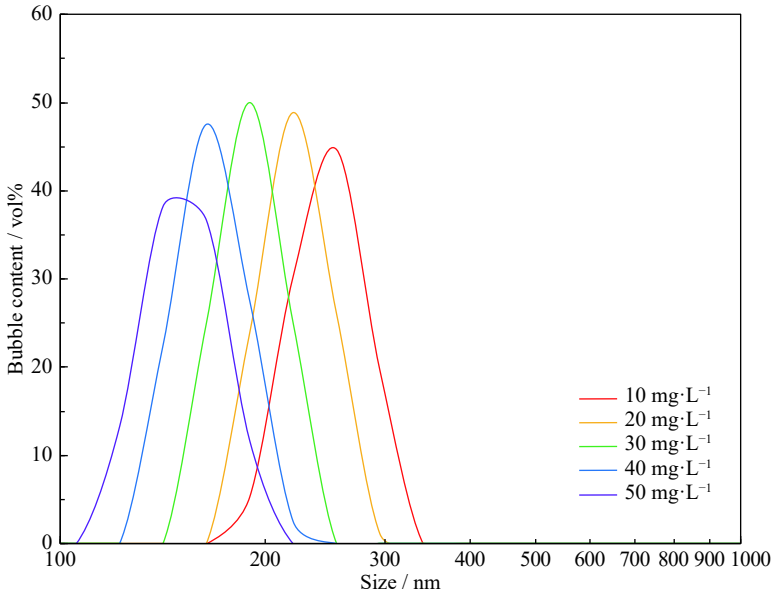

Fig. 2. Effect of MIBC dosage on the size distribution of nanobubbles (flow rate: 84.4 L/min; pH 6).

and Radke [40] proposed that, in pure water, bubbles are negatively charged mainly because of the special adsorption of OH^- at the gas–liquid interface. The change in potential is mainly due to the change in OH^- concentration in the solution, and the negative value of the surface potential increases with increasing OH^- concentration. When the concentration of nonionic surfactant increases gradually, OH^- and nonionic surfactant molecules compete for adsorption at the gas–liquid interface, reducing the gas–liquid interface potential.

3.2. Effect of the solution pH value on the nanobubble size and zeta potential

The electric double layer on the bubble surface plays an important role in the interaction between bubbles and the generation and stability of bubbles. The zeta potential is an important factor affecting electrostatic repulsion and should therefore be studied. Fig. 4 shows the change of the nanobubble size generated by the cavitation tube as a function of the pH value when the concentration of the MIBC surfactant was 50 mg/L. In this study, sodium hydroxide and hydrochloric acid were used to adjust the pH value. As evident from Fig. 4, the size of nanobubbles decreases consistently with increasing pH value. When the pH value increases from 3 to 12, the average diameter of nanobubbles decreases from approximately 620 to approximately 250 nm.

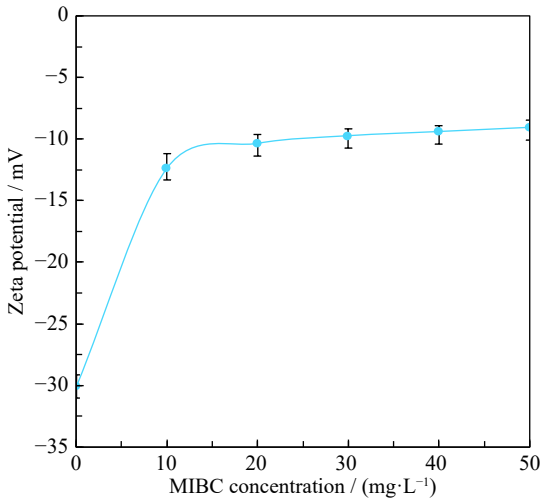

Fig. 3. Effect of MIBC concentration on the zeta potential of nanobubbles (flow rate: 84.4 L/min; pH 6).

Fig. 5 shows the relationship between the nanobubble zeta potential and size and pH value under the condition of 50 mg/L MIBC frother. Obviously, when the pH value was increased from 3 to 12, the zeta potential changed from a positive value to a negative value of −9 mV and the nanobubble size decreases from 652 to 251 nm. Elmahdy *et al.* [41] have reported that the bubble surface generated in water using nonionic frother MIBC has a negative charge. When the aqueous solution containing bubbles is alkaline, the concentration of OH^- in the solution also increases. Wu *et al.* [42] have shown that increasing the OH^- concentration in the aqueous bubble solution will increase the bubble surface charge and make the bubbles more stable through electrostatic repulsion. Obviously, the results in Fig. 5 show that higher pH values resulted in greater bubble surface charge, greater electrostatic repulsion, and, consequently, smaller bubbles. Calgaroto *et al.* [12] found that OH^- usually exists at the gas–liquid interface to form an electric double layer, which provides repulsive force and plays an important role in the generation and stability of bubbles.

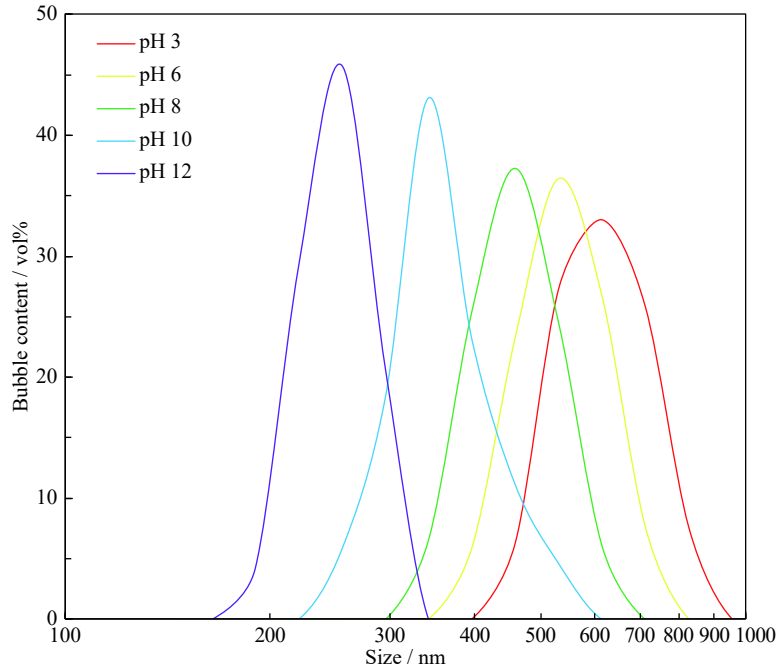

Fig. 4. Effect of the pH value on the average size distribution of nanobubbles (flow rate: 84.4 L/min; MIBC concentration: 50 mg/L).

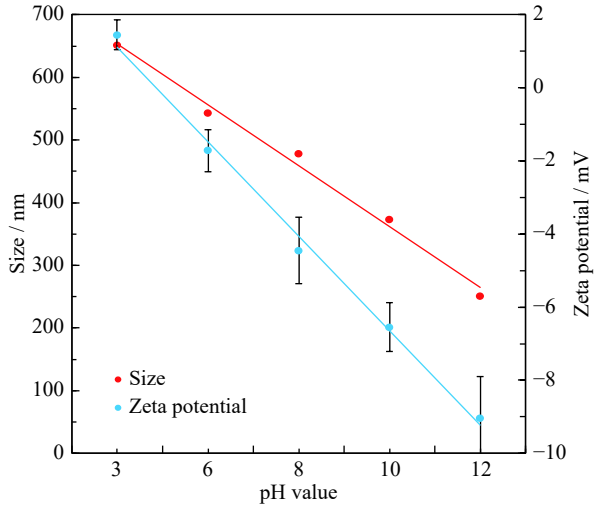

Fig. 5. Effect of the pH value on the average size and zeta potential of nanobubbles (flow rate: 84.4 L/min; MIBC concentration: 50 mg/L).

3.3. Effect of frother type on the zeta potential of nanobubbles

Fig. 6 shows the variation of the zeta potential of the surface of nanobubbles as a function of the solution pH value when 50 mg/L of the anionic surfactant sodium oleate ($C_{17}H_{13}COONa$) and the nonionic surfactants MIBC ($C_{16}H_{14}O$) and n-pentanol ($C_5H_{12}O$) was used, respectively.

The results in Fig. 6 show that, when the pH value was changed from acidic to alkaline, the surface potential of nanobubbles generated in the presence of sodium oleate was always negative, increasing from −2.08 mV at pH 3 to −38.8 mV at pH 12. When two nonionic frothers were used, the surface potential of the nanobubbles changed from positive to negative with increasing pH value of the solution and the difference in the surface potential values of the nanobubbles generated by the two agents was not obvious. The zeta potential was positive at pH 3 and became negative with increasing solution pH value. The zeta potential of bubbles changed from +1.04 mV to −9.04 mV and from +2.03 mV to −7.98 mV as the pH value was increased from 3 to 12 in the

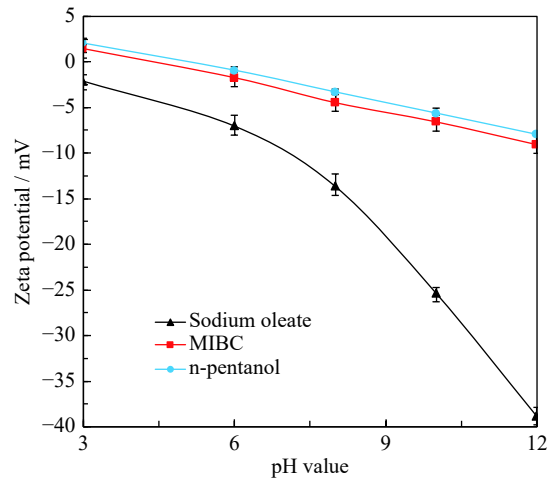

Fig. 6. Effect of the pH value on the zeta potential of nanobubbles generated using different types of frother (flow rate: 84.4 L/min; surfactant concentration: 50 mg/L).

presence of MIBC and n-pentanol, respectively. These results are in agreement with a previous study by Yoon and Yordan [43], who found that different surfactants produce different charges on bubbles. They also reported that anionic surfactants produce negatively charged bubbles and that nonionic surfactants produce negatively charged bubbles in the alkaline pH range and positively charged bubbles in the acidic pH range. They further noted that the structure of the nonionic surfactant affects the zeta potential of bubbles and that a higher oxygen/carbon (O/C) ratio in surfactant molecules may lead to a more negative zeta potential. The O/C ratios for MIBC and n-pentanol are 1/6 and 1/5, respectively; thus, the difference in zeta potential of bubbles generated by these two surfactants is not significant. Xiao *et al.* [44] recently investigated the pH effect on nanobubble zeta potential with and without sodium oleate and also likewise found that a higher pH value results in a more negative zeta potential and, more importantly, that the presence of sodium oleate increases the magnitude of the negative potential, suggesting selective adsorption of sodium oleate onto nanobubbles.

3.4. Influence of liquid flow rate on nanobubble size

Liquid flow rate is an important factor affecting liquid pressure and the hydrodynamic cavitation effect and will therefore affect the size of nanobubbles. Fig. 7 shows the change in nanobubble size, as measured with the cavitation tube, at different liquid flow rates in the presence of 30 mg/L frother.

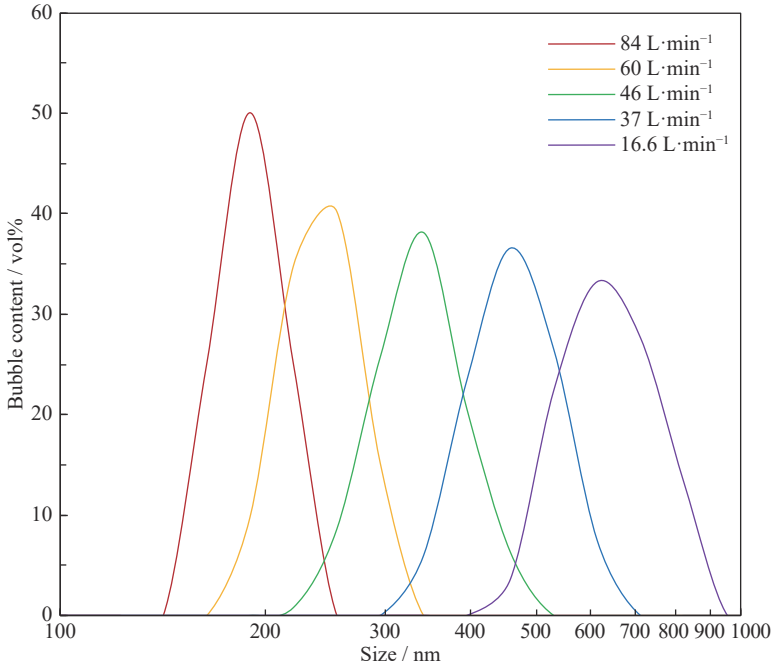

Fig. 7. Effect of liquid flow rate on the size distribution of nanobubbles (MIBC concentration: 30 mg/L; pH 6).

As evident from Fig. 7, the average size of nanobubbles decreases from 631 to 191 nm with increasing liquid flow rate from 16.6 to 84 L/min. Large quantities of microbubbles and nanobubbles were generated at high flow rates. However, when the flow rate was 16.6 L/min, very few microbubbles and nanobubbles were formed because of the low cavitation efficiency when the flow rate was too low. According to the Bernoulli equation,

$$P + \frac{1}{2}\rho U^2 = C \tag{1}$$

where P is the pressure, ρ the liquid density, U the liquid flow rate, and C is a constant. Rearranging Eq. (1) yields

$$U^2 + \frac{2P}{\rho} = \frac{2C}{\rho} \tag{2}$$

Therefore, when the liquid flow rate $U > \sqrt{\frac{2C}{\rho}}$, the pressure becomes negative and the cavitation tube is more prone to the cavitation effect. This equation shows that, when the liquid flow rate increases, the jet velocity increases, the impact strength between the jet fluid and the tube wall increases, and bubbles are more easily broken into smaller bubbles. Fujiwara *et al.* [45] postulated that a larger liquid flow rate implies a faster velocity through the throat of the cavitation tube, resulting in a sharp contraction and expansion of bubbles. When bubbles enter the throat, jet flow will occur. The jet flow increases the shear force on bubbles, increases the turbulence intensity in the expansion section, and is more likely to cause bubble fragmentation, thus making bubbles smaller. In general, increasing the flow rate of the

cavitation circulating liquid promotes the cavitation effect and the formation of micro- and nanobubbles.

3.5. Influence of air pressure on nanobubble size

The air content in a liquid strongly affects cavitation. Fig. 8 shows the effect of air pressure on the size distribution of nanobubbles when the frother concentration is 30 mg/L and the air flow rate is 0.1 L/min.

Fig. 8 shows that as the air pressure increases from 0.2 to 0.6 MPa, the nanobubble size increases from 248 to 581 nm. When the air pressure is low, the change in nanobubble size is obvious; however, when the air pressure exceeds a certain value, the change in nanobubble size is not obvious. Moreover, as the air pressure increases, the inlet pressure of the cavitation tube also increases. When the higher inlet pressure increases, the energy dissipation rate and turbulence intensity increase, thus intensifying cavity collapse and resulting in larger nanobubbles. Yang [46] found that, as the inlet pressure continues to increase, the jet flow area will also increase. Cavitation at this time will develop into supercavitation, resulting in a large number of cavitation bubbles forming a white mist of cavitation clouds. Water vapor near the wall will form a continuous phase containing dispersed liquid droplets, blocking the initiation of cavitation. In the blocking mode of cavitation, cavitation efficiency decreases, resulting in larger nanobubbles.

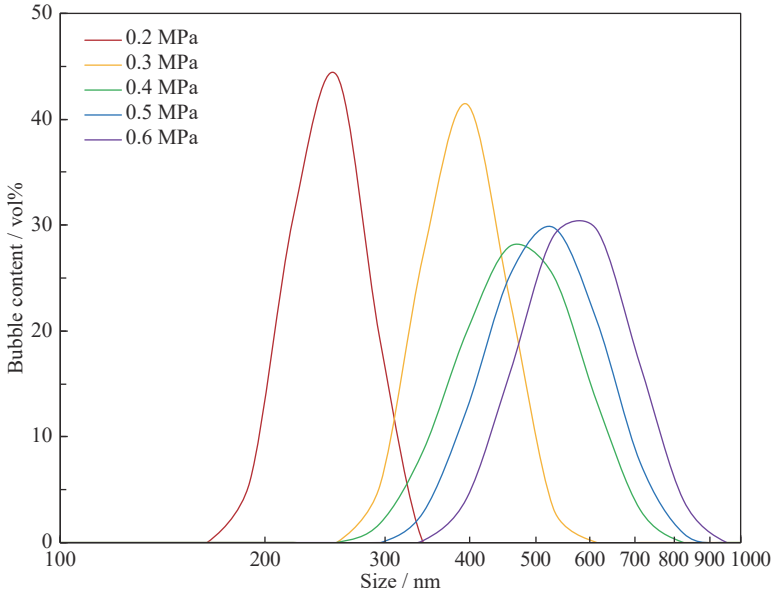

Fig. 8. Effect of air pressure on the size distribution of nanobubbles (MIBC concentration: 30 mg/L; liquid flow rate: 84 L/min; air flow rate: 0.1 L/min; pH 6).

3.6. Influence of air flow rate on nanobubble size

Fig. 9 shows the effect of different air flow rates on the size of nanobubbles when the frother concentration is 30 mg/L, the air pressure is 0.2 MPa, and the liquid flow rate is 84 L/min.

As the air flow rate was increased from 0.1 to 0.5 L/min, the average size of the nanobubbles gradually increases from 248 to 507 nm. Sada *et al.* [47] reported that at higher gas velocities, bubbles coalesced at a certain position from the nozzle and bubble diameter increased rapidly. Davidson and Amick [48] proposed an empirical expression for the initial bubble size of a single bubble:

$$V = 0.110\left(q \times r_{\mathrm{n}}^{0.5}\right)^{0.867} \tag{3}$$

where V is the volume of the bubble, q is the gas flow rate, and r_{n} is the nozzle radius. Therefore, for a given cavitation tube, the bubble volume increases with increasing gas flow rate. In the process of hydrodynamic cavitation, changes in gas solubility cause corresponding changes in the number and size of gas nuclei in the liquid, thus affecting the overall cavitation effect. During the cavitation development stage, the greater gas solubility will lead to more cavitation bubbles. However, in the subsequent cavitation stage, the greater gas solubility will cause more severe cavitation bubble collapse and decrease the number of cavities, resulting in a decrease in cavitation intensity. Fan *et al.* [23] demonstrated that, under the condition where other parameters are fixed, when oxygen or carbon dioxide is introduced during cavitation, the dissolved gas provides a large number of gas nuclei for nanobubble generation, thus enhancing cavitation. According to the Bernoulli equation, with increasing gas content, the par-

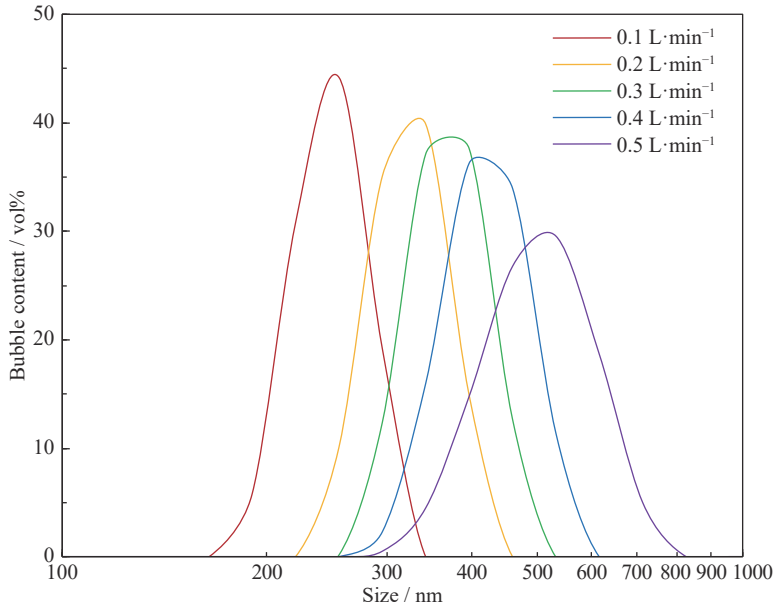

Fig. 9. Effect of air flow on the average size distribution of nanobubbles (MIBC concentration: 30 mg/L; liquid flow rate: 84 L/min; air pressure: 0.2 MPa; pH 6).

tial pressure of carbon dioxide or oxygen will also increase, which will reduce the pressure required to generate nanobubbles and lead to an increase of nanobubble size.

4. Conclusions

In this paper, the changes in the size distribution and surface zeta potential of bulk nanobubbles generated by hydrodynamic cavitation under different bubble generation conditions are studied. The following main conclusions were drawn from the research results:

(1) The size of nanobubbles generated by hydrodynamic cavitation is mostly distributed between 150 and 650 nm. A higher frother concentration, higher liquid flow rate, and higher pH value significantly reduce the size of nanobubbles.

(2) Frother concentration, pH value, and frother type substantially influence the zeta potential of nanobubbles. The frother molecules in the solution undergo competitive adsorption with OH^-, thus affecting the zeta potential.

(3) When the air pressure increases to a certain extent, hydrodynamic cavitation becomes supercavitation, which will further develop into hindered cavitation, where the cavitation efficiency decreases, resulting in an increase in the size of nanobubbles.

(4) Higher air flow rates provide a larger number of gas nuclei for the generation process of nanobubbles and may cause excessively violent cavitation and severe cavitation bubble collapse, resulting in a decrease in cavitation intensity and larger nanobubbles.

References

[1] M. Alheshibri, J. Qian, M. Jehannin, and V.S.J. Craig, A history of nanobubbles, *Langmuir*, 32(2016), No. 43, p. 11086.

[2] S.C. Li, *Cavitation of Hydraulic Machinery*, Imperial College Press, London, 2000, p. 32.

[3] Y. Xiong and F. Peng, Optimization of cavitation venturi tube design for pico and nano bubbles generation, *Int. J. Min. Sci. Technol.*, 25(2015), No. 4, p. 523.

[4] M.D Li, A. Bussonnière, M. Bronson, Z.H. Xu, and Q.X. Liu, Study of Venturi tube geometry on the hydrodynamic cavitation for the generation of microbubbles, *Miner. Eng.*, 132(2019), p. 268.

[5] W.G. Zhou, H. Chen, L.M. Ou, and Q. Shi, Aggregation of ultra-fine scheelite particles induced by hydrodynamic cavitation, *Int. J. Miner. Process.*, 157(2016), p. 236.

[6] W.G. Zhou, L.M. Ou, Q. Shi, Q.M. Feng, and H. Chen, Different flotation performance of ultrafine scheelite under two hydrodynamic cavitation modes, *Minerals*, 8(2018), No. 7, p. 264.

[7] D.P. Tao and A. Sobhy, Nanobubble effects on hydrodynamic interactions between particles and bubbles, *Powder Technol.*, 346(2019), p. 385.

[8] A. Sobhy and D.P. Tao, Effects of nanobubbles on froth stability in flotation column, *Int. J. Coal Prep. Util.*, 39(2019), No. 4, p. 183.

[9] N.K. Madavan, S. Deutsch, and C.L. Merkle, Reduction of turbulent skin friction by microbubbles, *Phys. Fluids*, 27(1984), No. 2, p. 356.

[10] H.Z. Li, L.M. Hu, D.J. Song, and F. Lin, Characteristics of micro-nano bubbles and potential application in groundwater bioremediation, *Water Environ. Res.*, 86(2014), No. 9,

p. 844.
[11] A. Agarwal, W.J. Ng, and Y. Liu, Principle and applications of microbubble and nanobubble technology for water treatment, *Chemosphere*, 84(2011), No. 9, p. 1175.
[12] S. Calgaroto, K.Q. Wilberg, and J. Rubio, On the nanobubbles interfacial properties and future applications in flotation, *Miner. Eng.*, 60(2014), p. 33.
[13] A. Sobhy and D. Tao, Nanobubble column flotation of fine coal particles and associated fundamentals, *Int. J. Miner. Process.*, 124(2013), p. 109.
[14] A.F. Rosa and J. Rubio, On the role of nanobubbles in particle–bubble adhesion for the flotation of quartz and apatitic minerals, *Miner. Eng.*, 127(2018), p. 178.
[15] S. Calgaroto, A. Azevedo, and J. Rubio, Flotation of quartz particles assisted by nanobubbles, *Int. J. Miner. Process.*, 137(2015), p. 64.
[16] K. Ebina, K. Shi, M. Hirao, J. Hashimoto, Y. Kawato, S. Kaneshiro, T. Morimoto, K. Koizumi, and H. Yoshikawa, Oxygen and air nanobubble water solution promote the growth of plants, fishes, and mice, *PLoS One*, 8(2013), No. 6, p. e65339.
[17] S. Cai, H. Shi, X.H. Pan, F.P. Liu, H.W. Xie, Y.Q. Xu, T. Xu, and N. Cao, Effects of micro-nano bubble aerated irrigation on water requirement characters and yield of double season rice, *Water Saving Irrig.*, 2017, No. 2, p. 12.
[18] X.T. Bao, Q.Y. Chen, Z.Q. Xu, D.D. Yue, R. Geng, and Y.L. Ding, Overview of research and application of micro-nano bubbles technology in fishery and aquaculture sector, *Water Purif. Technol.*, 35(2016), No. 4, p. 16.
[19] T.H. Li and H.Q. Lu, The energy dissipation rate per unit mass of jet pump mixture, *Mach. Dev.*, 2000, No. 4, p. 39.
[20] W.B. Cai, H.L. Yang, J. Zhang, J.K. Yin, Y.L. Yang, L.J. Yuan, L. Zhang, and Y.Y. Duan, The optimized fabrication of nanobubbles as ultrasound contrast agents for tumor imaging, *Sci. Rep.*, 5(2015), art. No. 13725.
[21] A.A. Kalmes, S. Ghosh, and R.L. Watson, A saline-based therapeutic containing charge-stabilized nanostructures protects against cardiac ischemia/reperfusion injury, *J. Am. Coll. Cardiol.*, 61(2013), No. 10, p. E106.
[22] R. Etchepare, H. Oliveira, M. Nicking, A. Azevedo, and J. Rubio, Nanobubbles: generation using a multiphase pump, properties and features in flotation, *Miner. Eng.*, 112(2017), p. 19.
[23] M.M. Fan, D. Tao, R. Honaker, and Z.F. Luo, Nanobubble generation and its applications in froth flotation (part I): nanobubble generation and its effects on properties of microbubble and millimeter scale bubble solutions, *Min. Sci. Technol. Chin.*, 20(2010), No. 1, p. 1.
[24] A.S. Najafi, J. Drelich, A. Yeung, Z.H. Xu, and J. Masliyah, A novel method of measuring electrophoretic mobility of gas bubbles, *J. Colloid Interface Sci.*, 308(2007), No. 2, p. 344.
[25] P.N. Rowe and R. Matsuno, Single bubbles injected into a gas fluidised bed and observed by X-rays, *Chem. Eng. Sci.*, 26(1971), No. 6, p. 923.
[26] Y.R. Tian, J.A. Ketterling, and R.E. Apfel, Direct observation of microbubble oscillations, *J. Acoust. Soc. Am.*, 100(1996), No. 6, p. 3976.
[27] J.S. Sung and J.M. Burgess, A laser-based method for bubble parameter measurement in two-dimensional fluidised beds, *Powder Technol.*, 49(1987), No. 2, p. 165.
[28] H. Tsuge, Y. Tanaka, and S.I. Hibino, Effect of the physical properties of gas on the volume of bubble formed from a submerged single orifice, *Can. J. Chem. Eng.*, 59(1981), No. 5, p. 569.
[29] R.T. Rodrigues and J. Rubio, New basis for measuring the size distribution of bubbles, *Miner. Eng.*, 16(2003), No. 8, p. 757.
[30] G.R. Caicedo, J.J.P. Marqués, M.G. Ruíz, and J.G. Soler, A study on the behaviour of bubbles of a 2D gas–solid fluidized bed using digital image analysis, *Chem. Eng. Process.*, 42(2003), No. 1, p. 9.
[31] Z.A. Zhou, N.O. Egiebor, and L.R. Plitt, Frother effects on bubble size estimation in a flotation column, *Miner. Eng.*, 6(1993), No. 1, p. 55.
[32] M.Y. Han, Y.H. Park, and T.J. Yu, Development of a new method of measuring bubble size, *Water Sci. Technol. Water Supply*, 2(2002), No. 2, p. 77.
[33] F.R. Young, *Cavitation*, McGraw-Hill Book Company, Maidenhead, 1989, p. 322
[34] R. Clift, J.R. Grace, and M.E. Weber, *Bubbles, Drops and Particles*, Academic Press, New York, 1978, p. 380.
[35] J.K. Edzwald, Principles and applications of dissolved air flotation, *Water. Sci. Technol.*, 31(1995), No. 3-4, p. 1.
[36] J.A. Finch, J.E. Nesset, and C. Acuña, Role of frother on bubble production and behaviour in flotation, *Miner. Eng.*, 21(2008), No. 12-14, p. 949.
[37] F. Azgomi, Characterizing frothers by their bubble size control properties [Dissertation], McGill University, Montreal, 2007, p. 14.
[38] A.K. Gupta, P.K. Banerjee, A. Mishra, P. Satish, and Pradip, Effect of alcohol and polyglycol ether frothers on foam stability, bubble size and coal flotation, *Int. J. Miner. Process.*, 82(2007), No. 3, p. 126.
[39] P. Moyo, C.O. Gomez, and J.A. Finch, Characterizing frothers using water carrying rate, *Can. Metall. Q.*, 46(2007), No. 3, p. 215.
[40] K.A. Karraker and C.J. Radke, Disjoining pressures, zeta potentials and surface tensions of aqueous non-ionic surfactant/electrolyte solutions: theory and comparison to experiment, *Adv. Colloid Interface Sci.*, 96(2002), No. 1-3, p. 231.
[41] A.M. Elmahdy, M. Mirnezami, and J.A. Finch, Zeta potential of air bubbles in presence of frothers, *Int. J. Miner. Process.*, 89(2008), No. 1-4, p. 40.
[42] C.D. Wu, K. Nesset, J. Masliyah, and Z.H. Xu, Generation and characterization of submicron size bubbles, *Adv. Colloid Interface Sci.*, 179-182(2012), p. 123.
[43] R.H. Yoon and J.L. Yordan, Zeta-potential measurements on microbubbles generated using various surfactants, *J. Colloid Interface Sci.*, 113(1986), No. 2, p. 430.
[44] W. Xiao, Y.L. Zhao, J. Yang, Y.X. Ren, W. Yang, X.T. Huang, and L.J. Zhang, Effect of sodium oleate on the adsorption morphology and mechanism of nanobubbles on the

mica surface, *Langmuir*, 35(2019), No. 28, p. 9239.
[45] A. Fujiwara, K. Okamoto, K. Hashiguchi, J. Peixinho, S. Takagi, and Y. Matsumoto, Bubble breakup phenomena in a venturi tube, [in] *ASME/JSME 2007 5th Joint ASME/JSME Fluids Engineering Conference*, California, 2007, p. 1.
[46] H.Z. Yang, *Experimental Study on Enhancive Effect of Hydrodynamic Cavitation* [Dissertation], Dalian University of Technology, Dalian, 2006, p. 36.
[47] E. Sada, A. Yasunishi, S. Katoh, and M. Nishioka, Bubble formation in flowing liquid, *Can. J. Chem. Eng.*, 56(1978), No. 6, p. 669.
[48] L. Davidson and E.H. Amick, Formation of gas bubbles at horizontal orifices, *AIChE J.*, 2(1956), No. 3, p. 337.